

# A Fatigue Crack Initiation Map for Polycarbonate

T.-J. CHEN,<sup>1</sup> C. P. BOSNYAK,<sup>2</sup> C.-I. KAO, and A. CHUDNOVSKY<sup>1,\*</sup>

<sup>1</sup>Department of Civil Engineering, Mechanics and Metallurgy, University of Illinois at Chicago, P.O. Box 4348, Chicago, Illinois 60680, and <sup>2</sup>The Dow Chemical Company, Polycarbonate R&D, B-1470A, 2301 N. Brazosport Blvd., Freeport, Texas 77541

## SYNOPSIS

The mechanisms of fatigue crack initiation for various stress levels and thicknesses have been determined for single-edge notched specimens of polycarbonate and used to assemble a map. Three basic fatigue crack initiation mechanisms were identified and named as cooperative ductile (the damage zone formed ahead of crack consisting of yielded material), solo-crack brittle (very little damage zone development), and cooperative brittle (identified as a cloud of microcracks or crazes that developed at the notch tip). With a given applied stress and within the same failure mechanism, the values of the number of cycles to crack initiation decrease with increase in thickness. The transition from cooperative ductile to solo-crack brittle initiation mechanisms is sudden with increasing thickness. Transition from cooperative ductile to cooperative brittle with decreasing stress was less well defined. Regions where combinations of mechanisms were observed are also identified in the map.

© 1993 John Wiley & Sons, Inc.

## INTRODUCTION

Today, there are increasing demands placed upon polymers for use in durable structural applications. The problem is that there are no established models for which design engineers can predict time to failure, even under the simplest of loading conditions. The basic progressive stages of failure can be considered as incubation, leading to crack initiation, stable or controlled crack growth, then unstable or uncontrolled crack propagation. Much effort has been placed in the fracture community toward studies of crack propagation,<sup>1</sup> but relatively little has been placed on the initiation problem. A requirement for the prediction of service lifetime is the development of suitable criteria for the three basic stages. Following is a brief review of the development of criteria, first for strength of materials, then for fracture toughness.

The history of the strength of materials goes back many centuries but was not formalized until over 300 years ago when Galileo proposed a simple critical

loading criterion for failure. From there followed a steady increase in the number of proposed criteria for strength based on components of stress or strain tensors, so that today there are many variants of such criteria.<sup>2</sup> Clearly, this large number of strength criteria reflects the basic lack of fundamental understanding of the conditions for failure. The relatively recent developments of failure mechanism maps dispel the naive concept of a single universal criterion for strength and represent the present level of understanding and characterization of the strength of materials.<sup>3-6</sup> The axes usually chosen are applied stress normalized by the modulus and temperature normalized by either the melting point or the glass transition temperature. Using data from Bauwens-Crowet et al.,<sup>4</sup> a fracture mechanism map for poly(bisphenol A carbonate) of  $M_w$  35,000 g/mol in simple tension and compression for several strain rates and temperatures was developed by Bin Ahmad and Ashby.<sup>5</sup> Polycarbonate is well known for its impact toughness. Various regimes as elastic, plasticity and yielding, adiabatic heating, rubbery flow, and viscous flow were identified. They further attempted to fit data from poly(methyl methacrylate), polystyrene, polyisobutylene, a cross-linked epoxy, and polycarbonate (PC) to simplified con-

\* To whom correspondence should be addressed.

stitutive equations for each regime.<sup>5</sup> The main message gained from fracture mechanism maps is that there are various modes of failure, each of which require, consequently, their own specific strength criterion.

Since the 1950s it became obvious that fracture toughness, defined as the resistance to crack initiation and growth, is another material property that is as important, if not more so, than strength for practical application. Fracture toughness is usually described in terms of a critical stress intensity factor ( $K_{1c}$ ), critical crack-tip opening displacement (CCTOD), critical energy release rate ( $G_{1c}$ ,  $J_{1c}$ ), etc. It is interesting to note the parallel of thought in the development of critical toughness criteria with those of critical strength criteria. Unfortunately, it appears that the lessons gained from the evolution of strength criteria were not fully appreciated in the development of fracture toughness criteria. In both cases, they have the same inherent limitations due to the lack of consideration of the effects of time. An example of a fatigue fracture mechanism map for plastics was developed by Takemori for an injection-molded PC of molecular weight,  $M_w$ , of 53,900.<sup>6</sup> In these particular experiments, the notch was introduced through the formation of a weldline and the tensile yield stress,  $\sigma_y$ , and glass transition temperature,  $T_g$ , were chosen for normalization. Three basic modes of failure were identified by Takemori for the tension-tension fatigue of PC: (i) necking with applied stresses close to  $\sigma_y$  at a given temperature, (ii) shear banding at intermediate stresses and temperatures, and (iii) crazing at low stresses and temperatures less than 70°C.

In this article we have begun the process of understanding failure initiation of a PC by first attempting to classify the various failure initiation mechanisms available to this material in tension-tension fatigue. Here, we are determining the effects of varying stress level and thickness of PC using single-edge notched specimens. The range of thickness examined, 0.2–4.0 mm, was selected based on actual common utility of PC. We will show our first attempt at the development of a fatigue failure initiation mechanism map. We emphasize that it leaves much room for further development through appropriate normalization of the axes.

## EXPERIMENTAL

### Material, Specimen Preparation, and Testing

Polycarbonate, molecular weight,  $M_w$ , 29,000 g/mol, was kindly provided by the Dow Chemical Co. in

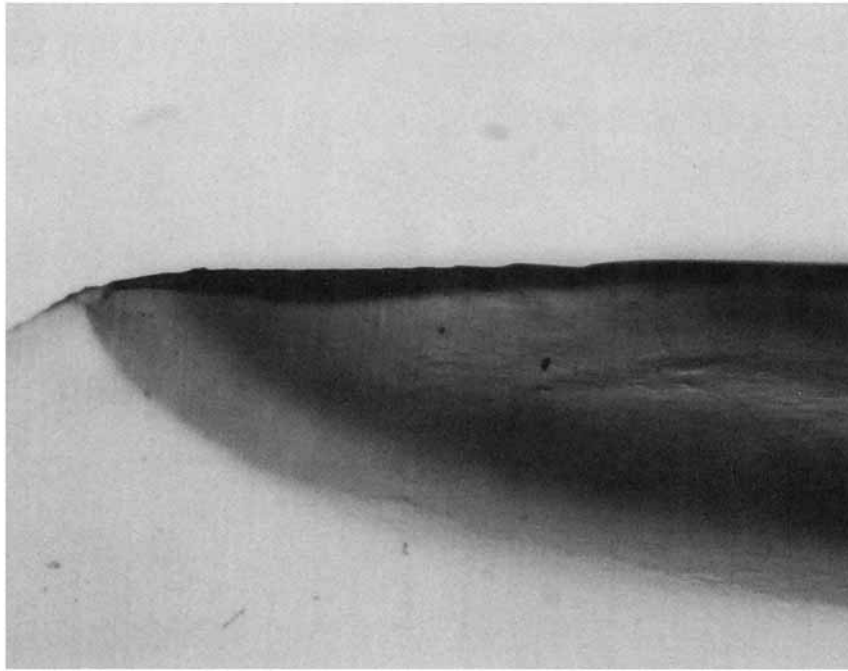
the form of injection-molded plaques of 3.1 and 6.2 mm thickness. After drying in a vacuum oven at 130°C for 24 h, the plaques were further compressed to smaller thickness using a Duke compression molder under the following conditions: Preheated to 240°C under no load for 10 min, under 30 tons ram pressure for 20 min, then cooled to 200°C by air, followed by water to 30°C, while still maintaining pressure. Rectangular specimens 80 × 20 mm were cut from the sheets and a 60° V-notch milled into the center of one long edge with notch length 1 mm and notch radius 0.01 mm. For tensile testing, dumbbell-shaped specimens of gauge length 50 × 10 mm were machined from the 3.1 mm plaques and pulled at an initial strain rate of 0.02% s<sup>-1</sup>. The tensile yield stress,  $\sigma_y$ , was determined as 68 MPa. Generally, three specimens were tested at each condition except with thicknesses 1.2 and 1.4 mm, where at least 16 specimens were examined at  $\sigma_{max}/\sigma_y = 0.45$ .

The tension-tension fatigue experiments were conducted on a 1.1 ton capacity servohydraulic Instron Testing System at room temperature. Sinusoidal waveform loading with frequency of 1.0 Hz was used for fatigue testing. The range of stress levels was ( $\sigma_{max}/\sigma_y$ ) 0.35–0.75 and minimum-to-maximum stress ratio,  $R(\sigma_{min}/\sigma_{max}) = 0.4$ .

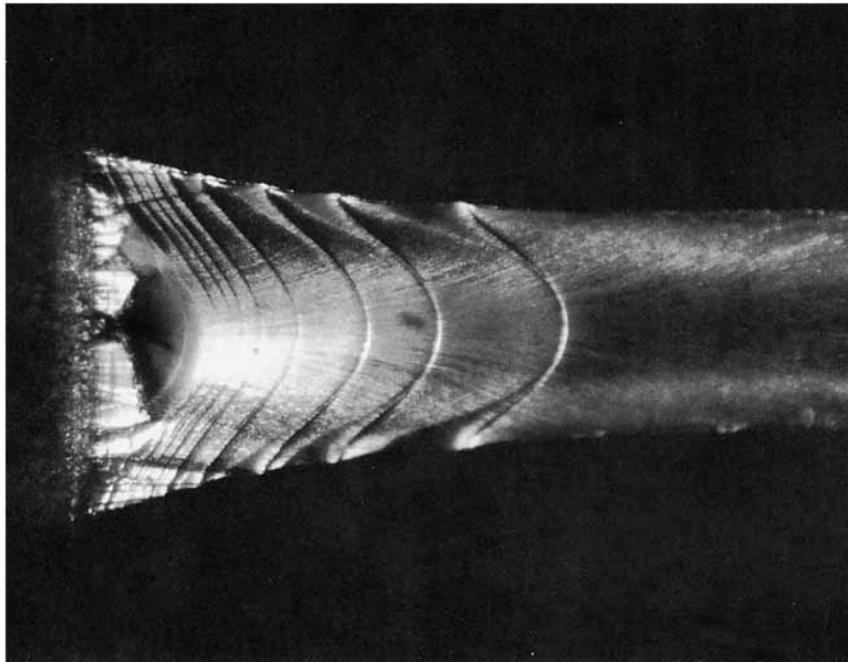
The crack and surrounding damage was followed using a traveling optical microscope attached to a video camera. This assembly is equipped with a visual display unit from which the entire history of crack propagation is analyzed. Postfracture optical observations are performed on a Zeiss light microscope. For evaluation of the number of cycles to crack initiation,  $N_i$ , under the various conditions, the crack is considered to have initiated when it reached 0.2 mm from the notch on the specimen surface. This convention was adapted for ease of detection of the crack and, hence, for consistency of measurement with duplicate specimens. The thinning ratio at a given crack length is defined as  $(Z_0 - Z)/Z_0$ , where  $Z_0$  is the initial thickness, and  $Z$ , the fracture surface thickness.

## RESULTS AND DISCUSSION

In Figures 1–5 are shown the side view and fracture surfaces as viewed optically at 50× magnification of the various thickness specimens of PC subjected to five different loading conditions. From these pictures, we can identify three basic mechanisms and two combinations of mechanisms. A typical example of *cooperative ductile* is seen in Figure 1, which is

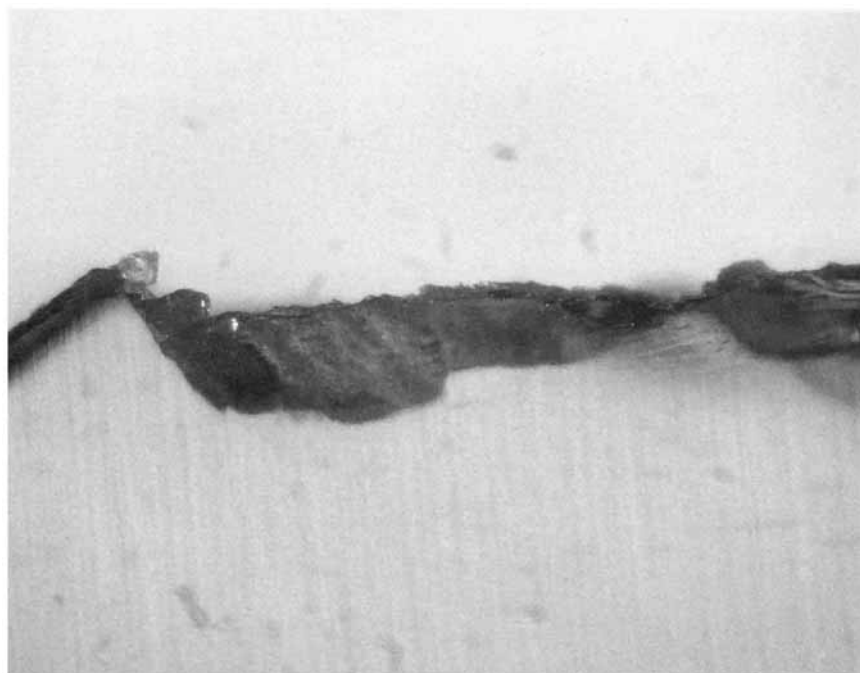


0.2 mm

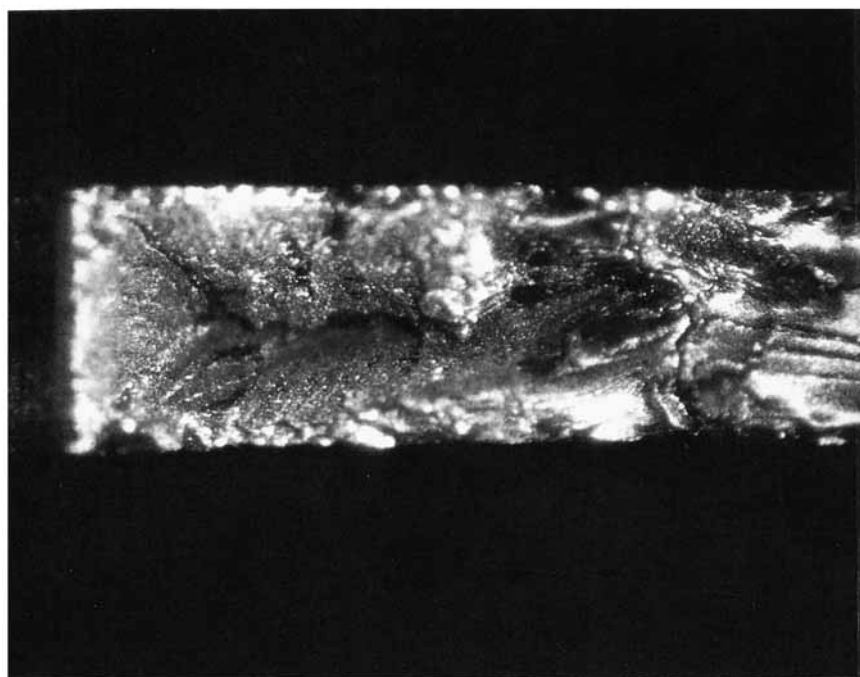


0.2 mm

**Figure 1** Cooperative ductile fatigue failure initiation in PC:  $\sigma_{\max}/\sigma_y = 0.75$ ; thickness 1.0 mm.

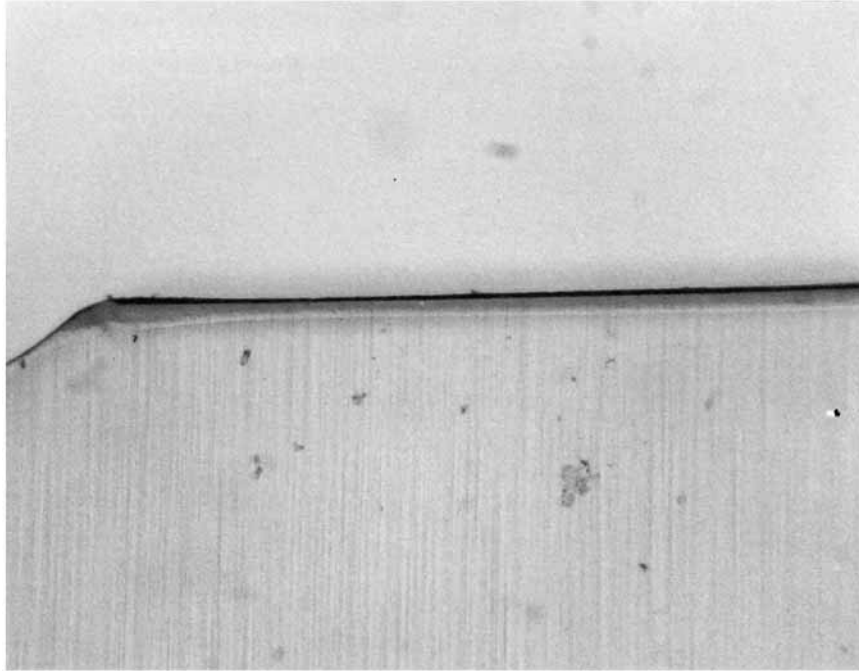


0.2 mm

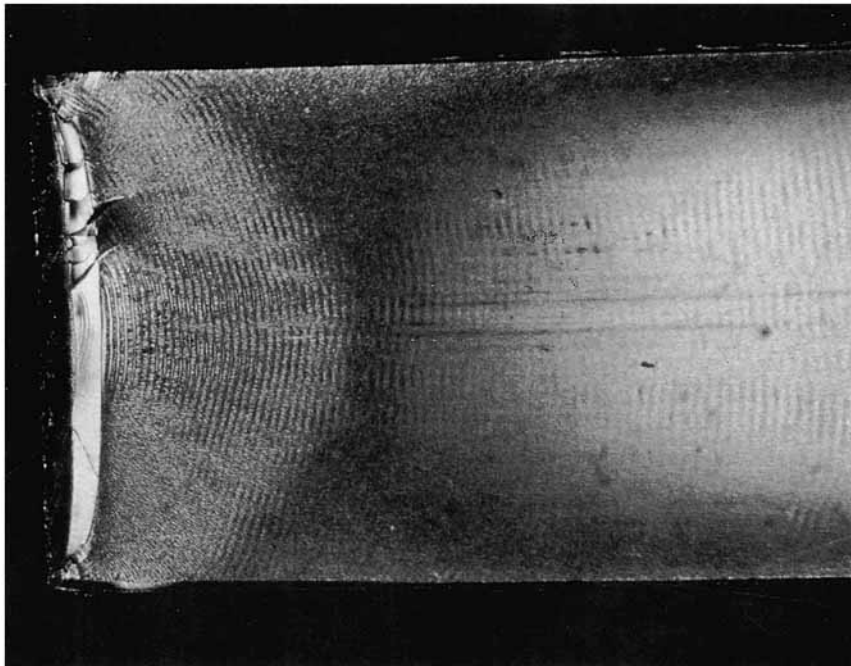


0.2 mm

**Figure 2** Cooperative brittle fatigue failure initiation in PC:  $\sigma_{\max}/\sigma_y = 0.35$ ; thickness 0.7 mm.

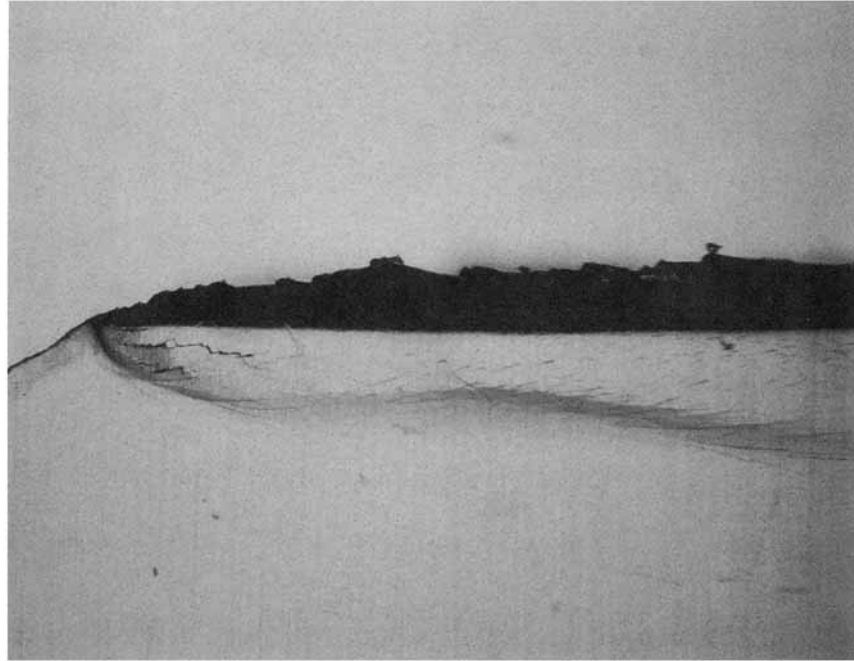


0.2 mm

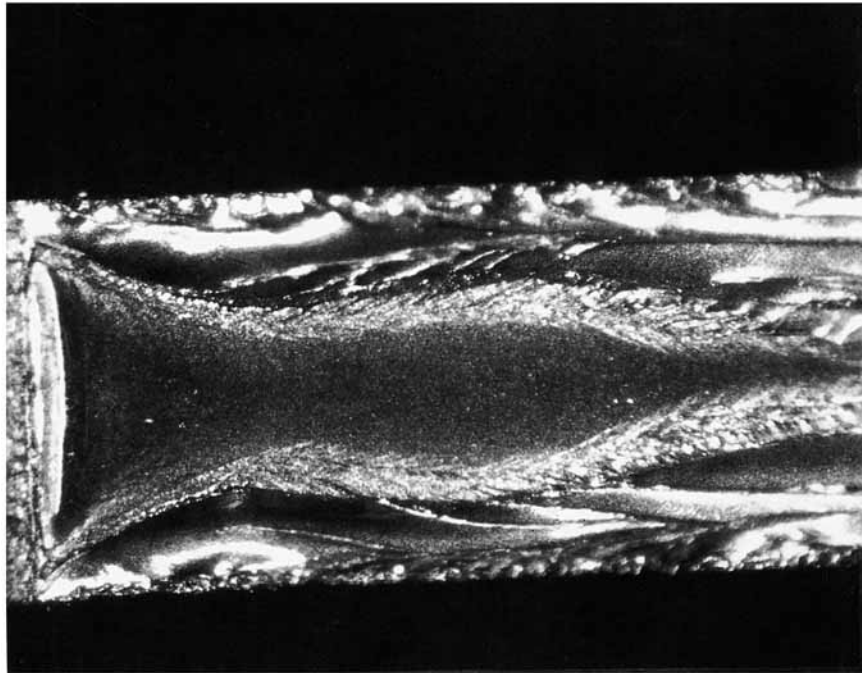


0.2 mm

**Figure 3** Solo-crack brittle fatigue failure initiation in PC:  $\sigma_{\max}/\sigma_y = 0.35$ ; thickness 1.4 mm.

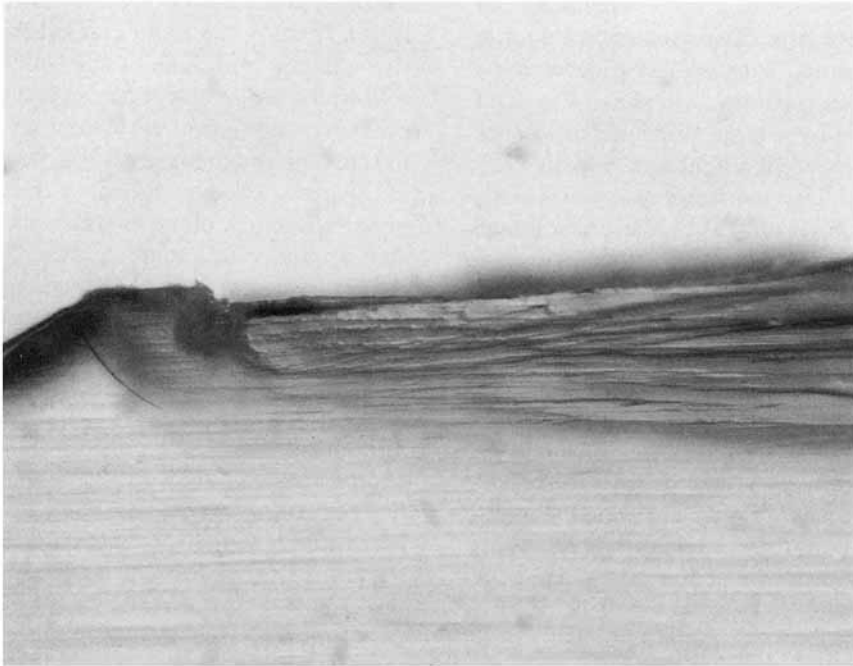


0.2 mm

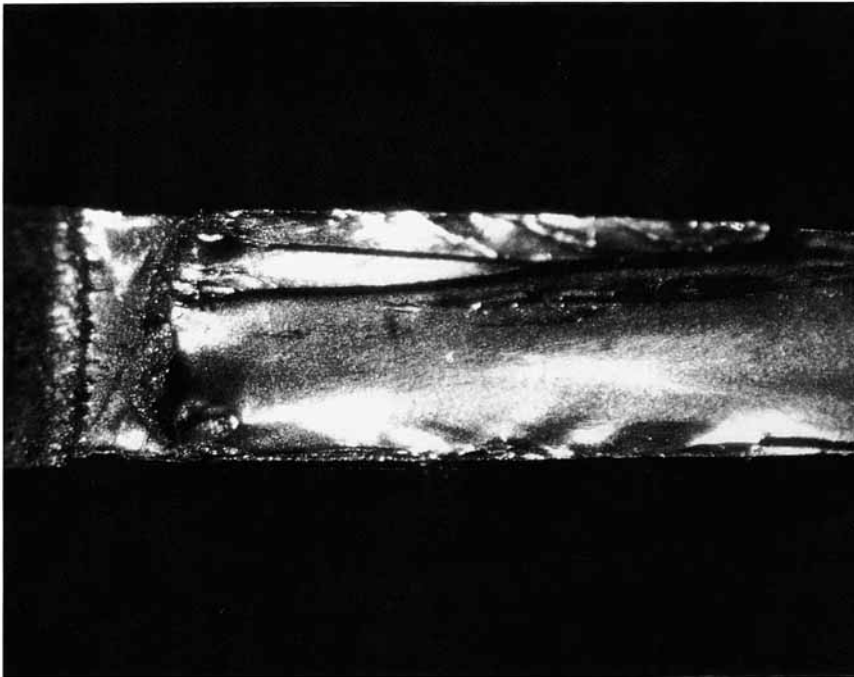


0.2 mm

**Figure 4** Mixed cooperative brittle and solo-crack fatigue failure initiation in PC:  $\sigma_{max}/\sigma_y = 0.35$ ; thickness 1.0 mm.



0.2 mm



0.2 mm

**Figure 5** Mixed cooperative brittle and cooperative ductile fatigue failure initiation in PC:  $\sigma_{\max}/\sigma_y = 0.55$ ; thickness 0.7 mm.

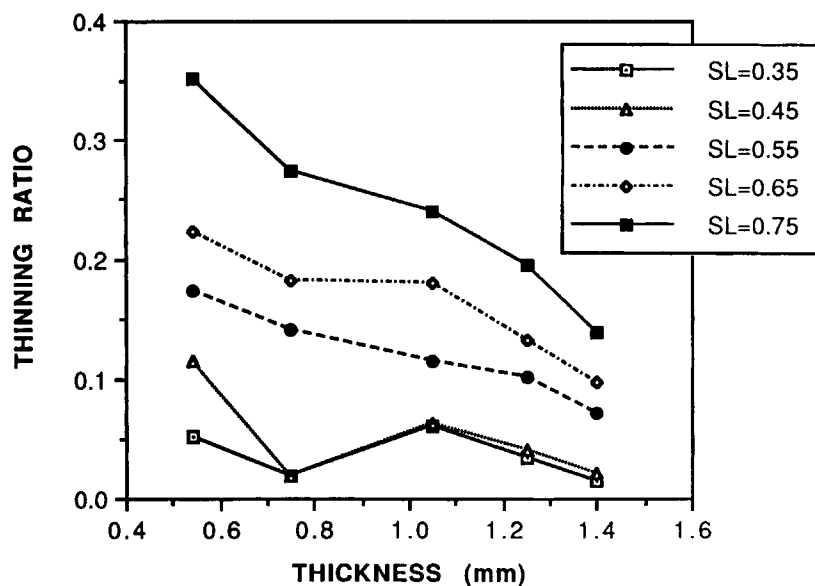
obtained at stress levels  $\sigma_{\max}/\sigma_y > \sim 0.5$  for all thicknesses examined here. The cooperative ductile mechanism is so named because the process zone associated with crack initiation consists of yielded material as reflected by a large thinning ratio and, hence, representative of significant cooperative deformation processes. This mechanism appears analogous to necking behavior in PC.<sup>6,7</sup> The crack grows through the midplane of the damage zone, which is expected based on the symmetry of loading and geometry.

Figure 2 shows a representative fracture surface around the notch from the side and top views of specimens tested at  $\sigma_{\max}/\sigma_y < 0.45$  and thicknesses of 0.2–0.7 mm. In spite of the symmetry of the loading and specimen geometry, the process zone was observed to develop asymmetrically. Furthermore, the process zone apparently consists of a large number of microcracks or crazes, and so we call the mechanism of initiation *cooperative brittle*. At this scale of magnification, we were unable to determine whether these microfeatures were actually crazes as suggested by Takemori<sup>6</sup> or cracks as described by Sehanobish et al.<sup>8</sup> Some of this discrepancy could be ascribed to the effect of PC molecular weight; Takemori examined PC with an  $M_w$  of 59,000; Sehanobish et al., of 35,000; and ourselves, of 29,000 g/mol. Accordingly, we expect our observations to be more similar to those observations by Sehanobish et al., i.e., to develop microcracks. The microcracks were observed to develop along the lines expected

of the principal stress trajectories. It was noted that in many cases the main crack did not grow initially through the midplane of the process zone, but also followed a curved path through the initially formed process zone before returning to the plane of the notch. The rough nature of the fracture surface seen in Figure 2 clearly indicates that the main crack grew through a cloud of microcracks. We suggest that an important role is played by the statistics of critical defects that triggers the microcrack formation and subsequent crack initiation.

Figure 3 illustrates an example of a mechanism that we have named *solo-crack brittle* at low stress levels  $\sigma_{\max}/\sigma_y < 0.45$  and high thickness  $> 1.2$  mm. Solo-crack brittle is a well-known failure mechanism of cross-linked polymers such as epoxies<sup>9,10</sup> with very little thinning. As the name suggests, only one crack is initiated, which propagates immediately within one cycle to give ultimate part failure. Consequently, the surface is seen to be "mirrorlike" with a very small process zone at the corners of the notch tip. In a manner similar to cooperative ductile, the crack grows through the plane of the notch tip.

Some of the mechanisms are seen to be competing with each other under certain intermediate conditions. For example, in Figure 4 are shown the side and top views of PC subjected to  $\sigma_{\max}/\sigma_y$  of 0.35 and of thickness 1.0 mm. On the outer fracture surfaces of the specimen are observed the characteristics of cooperative brittle, whereas in the core of the specimen, a flat planar surface, solo-crack brittle, is seen.



**Figure 6** Thinning ratios at 0.2 mm surface crack length vs. thickness of the PC for  $\sigma_{\max}/\sigma_y$  of 0.35–0.75.



In contrast to the core fracture surface, the fracture surface of the sides of the specimen were not in the plane of the notch tip. There is little thinning of the specimen. Figure 5 illustrates an example of mixed cooperative brittle and cooperative ductile failure at  $\sigma_{\max}/\sigma_y$  0.55 and thickness 0.7 mm. Within about 0.15 mm of the notch tip are observed the dominant features of cooperative brittle. However, a struggle between the failure mechanisms is evident, and thereafter ductile drawing is dominant.

The thinning ratios show the contribution of ductility in the specimens subjected to the various conditions. In Figure 6 are the thinning ratios (determined from the optical micrographs at 0.2 mm surface crack length) vs. thickness of the PC for the stress levels examined. The reduction in ductility with decreasing stress level and increasing thickness is clearly seen. These results are in good agreement with previous observations of the thinning ratio of various thicknesses of PC tested in fatigue.<sup>8</sup> The increase in ductility with decreasing thickness is to be expected based on simple plane strain to plane stress considerations.<sup>11</sup> The thinning ratios are to be used in the future to quantify the energies involved in process zone evolution.

In Figure 7 is plotted the number of fatigue cycles to initiate the 0.2 mm surface crack,  $N_i$ , vs. thickness of the sheets at the various stress levels examined. The error bars represent the scatter of  $N_i$  determined on 16 identical specimens. Generally, the values of  $N_i$  at a given test condition were within a

factor of 3. Some scatter in  $N_i$  with specimens of intermediate thicknesses arose from our method of determining crack growth from the surface because some crack tunneling was observed. From a general perspective, the values of  $N_i$  decrease with increase in thickness and increasing stress levels. Of importance, these results differ from those obtained with higher molecular weight PC ( $M_w$  35,000 g/mol) where the values of  $N_i$  at  $\sigma_{\max}/\sigma_y = 0.5$  increased with increasing thickness while maintaining a cooperative ductile failure mechanism.<sup>8</sup> The sensitivity of the failure mechanisms to PC molecular weight is well known for impact failures<sup>12,13</sup> and several molecular weight PCs are presently being examined in fatigue in our laboratories.

It is useful to see the relationships among stress level, the time to initiate a crack, and the thickness of the sheet in regard to the failure mechanism. In figure 8 is plotted the normalized applied stress vs.  $\log(N_i)$  for the various thicknesses denoted. The solid lines represent the connection of experimental data of the same failure initiation mechanism. The dashed lines represent the extension of a single mechanism, and the dotted lines, a transition in mechanism. To some extent, this is similar to an approach taken by Takemori using total number of cycles to full part fracture.<sup>6</sup> Our observations are that the value of  $N_i$  for a given failure mechanism increases with decreasing applied stress and decreases with increasing sheet thickness. With thickness greater than 1.2 mm, the number of cycles to

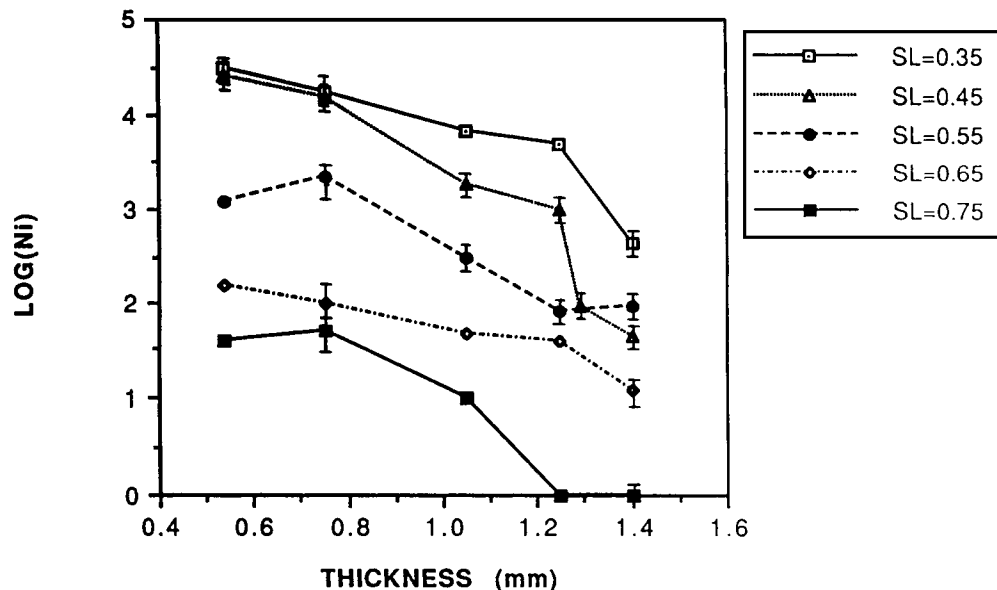
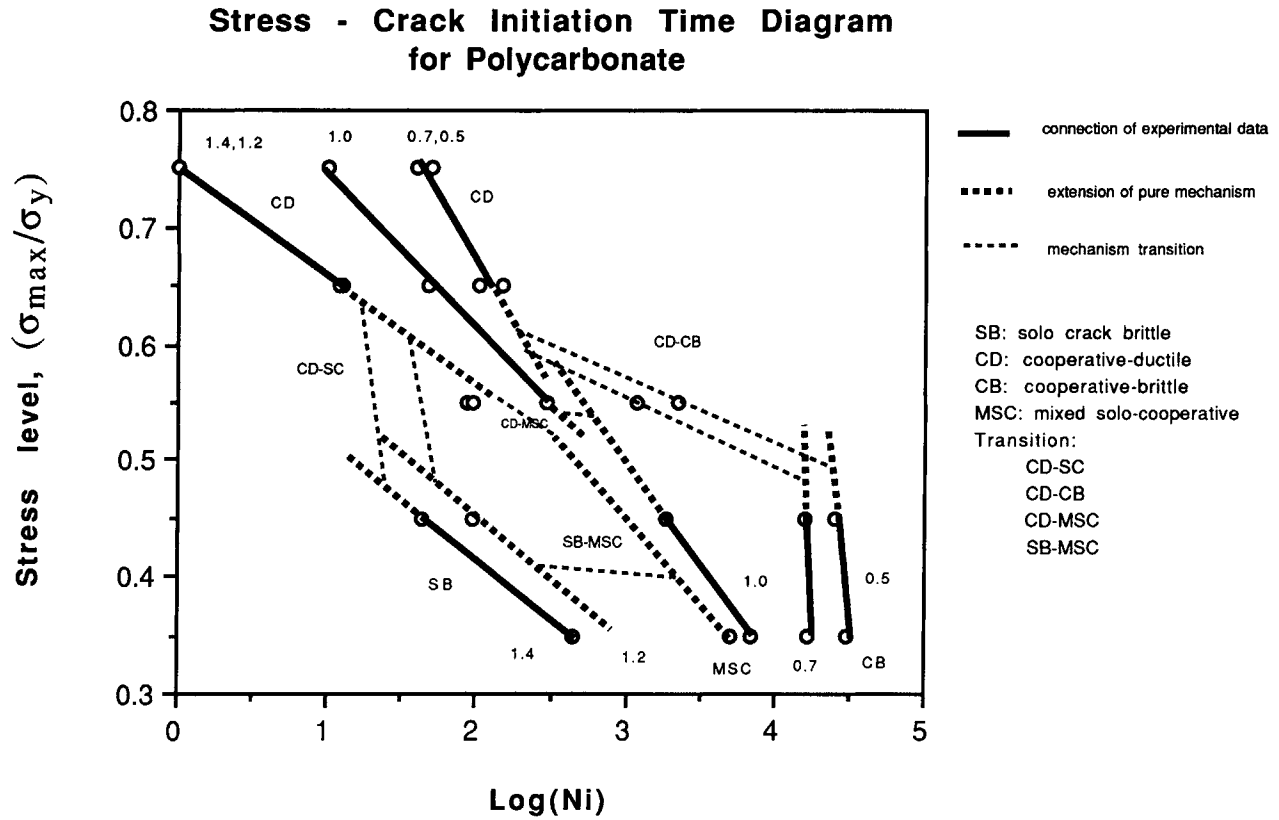
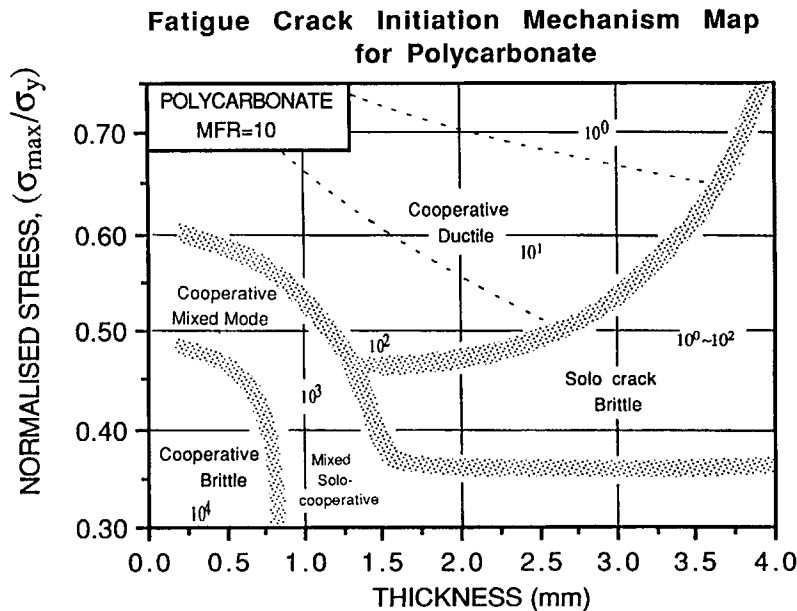


**Figure 7** Number of fatigue cycles to initiate the 0.2 mm surface crack,  $N_i$ , vs. thickness of the sheets at  $\sigma_{\max}/\sigma_y$  of 0.35–0.75.



initiate a crack underwent an inversion with decreasing stress levels at the point of change in mechanism from cooperative ductile to solo-crack

brittle. The transition in initiation mechanisms from cooperative ductile to solo-crack brittle is very sudden with increasing thickness, whereas transition



from cooperative ductile to cooperative brittle is less well defined. This latter phenomenon is similar to that observed in the fracture toughness evaluation of PC.<sup>13,14</sup>

In Figure 9 is given our first attempt of a fatigue crack initiation mechanism map for PC. The normalized applied stress is plotted against the thickness of the specimen. The orders of values of  $N_i$  are also shown in the plot. Attempts to use the stress intensity factor to normalize the loading conditions were made by changing the initial crack length from 1.0 mm to 0.5 and 2.0 mm. In some cases, the same initial values of the stress intensity gave different initiation mechanisms and so could not be used. As has been done elsewhere, the thickness of the sheet could be normalized against the plastic zone size calculated according to the well-known Dugdale-Barenblatt model.<sup>15</sup> However, this approach was also abandoned based on the lack of additional knowledge that it provided. It appears somewhat arbitrary in our case whether one selects the plastic zone size solution for plane stress or plane strain; the essential features of the map remain.

## CONCLUSIONS

1. Novel fatigue crack initiation mechanisms maps are under development for engineering polymers. An illustrative example with polycarbonate is given where the effects of thickness (0.5–4 mm) and applied tensile loading at frequency 1 Hz on single-edge notched specimens are examined.
2. The number of fatigue cycles to initiate a crack were found strongly dependent on the micromechanism of deformation that occurs at the notch tip prior to crack formation and, hence, not to be a simple function of the applied stress.
3. Three basic fatigue crack initiation mechanisms were identified and named here as cooperative ductile (at high stresses, the damage zone formed ahead of crack consisting of yielded material), solo-crack brittle (at large thicknesses, very little damage zone development), and cooperative brittle (identified as a cloud of microcracks that developed at the notch tip at low stresses in thin speci-

mens). Increasing ductility was observed with decreasing thickness and applied stresses close to the tensile yield stress, but the changeover in mechanism with change in applied stress was much more dramatic for the thicker specimens.

The authors wish to thank Dr. A. Kim, University of Illinois at Chicago, and Dr. K. Sehanobish, The Dow Chemical Co., for their helpful discussions. Thanks also to E. Garcia-Meitin, The Dow Chemical Co., for the photomicrographs and The Dow Chemical Co. for the financial support of this work.

## REFERENCES

1. A. Moet, in *Failure of Plastics*, W. Brostow and R. D. Corneliusen, Eds., Hanser, New York, 1986, Chap. 18.
2. H. Libowitz, *Fracture*, Academic Press, New York, 1968, Vol. II.
3. M. F. Ashby, C. Gandhi, and D. M. R. Taplin, *Acta Metal.*, **27**, 699 (1979).
4. C. Bauwens-Crowet, J. C. Bauwens, and G. A. Homes, *J. Mater. Sci.*, **7**, 176 (1972).
5. Z. Bin Ahmad and M. F. Ashby, *J. Mater. Sci.*, **23**, 2037 (1988).
6. M. T. Takemori, *Polym. Sci. Eng.*, **28**, 641 (1988).
7. J. W. Maher, R. N. Haward, and J. N. Hay, *J. Polym. Sci.*, **18**, 2169 (1980).
8. K. Sehanobish, N. Haddaoui, and A. Moet, *J. Mater. Sci.*, to appear.
9. A. J. Kinloch, *Adv. Polym. Sci.*, **72**(19), 46–67 (1980).
10. A. Chudnovsky, A. Kim, and C. P. Bosnyak, *Int. J. Fract.*, **55**, 209 (1992).
11. J. F. Knott, *Fundamentals of Fracture Mechanics*, Butterworths, London, 1973.
12. *Properties of Calibre Resins*, Promotional literature available from The Dow Chemical Company, 1990.
13. F.-C. Chang and H.-C. Hsu, *J. Appl. Polym. Sci.*, **43**, 1025 (1991).
14. K. Sehanobish, D. H. Bank, and C. P. Bosnyak, *Advances in Fracture Research*, K. Salama, K. Ravi-Chandar, D. M. R. Taplin, and P. Rama Rao, Eds., Pergamon Press, New York, 1989, Vol. 4, p. 2789.
15. M. Parvin and J. G. Williams, *Int. J. Fract.*, **11**, 963 (1975).

Received September 15, 1992

Accepted January 14, 1993